SOME PHYSICO-OPTICAL CHARACTERIZATION OF BULK CHALCOGENIDES OF THE $(As_4S_3Se_3)_{1-x}:Sn_x$

O.V. Iaseniuc, M.S. Iovu, E.P.Colomeico, E. Harea,
Institute of Applied Physics, Academy of Sciences of Moldova
5 Academiei str., MD-2028 Chisinau, Republic of Moldova
oxygena08@rambler.ru

Absract: The experimental results of an investigations of the microhardness of the surfaces dependence of glasses composition; optical transmission in the visible and near infrared (IR) regions and Raman spectra of bulk samples of $(As_4S_3Se_3)_{1-x}:Sn_x$ glasses with $x = 0 \div 10$ at.% are obtained and discussed. It was established that the addition of such amounts of tin don't leads to essentially changes in the glass physical properties, such as values of the stress and Young's modulus related to the modification of the density and compactness. The XRD measurements showed that the Sn impurities in the $(As_4S_3Se_3)_{1-x}:Sn_x$ essentially don't change the shape of the first sharp diffraction peak (FSDP) of the X-ray diffraction patterns, the intensity and the position of the FSDP non-monotoniously depend on the Sn concentration. However the doping of $As_2(S, Se)_3$ chalcogenide glass with tin impurities essentially reduces the absorption bands of S-H (Se-H) and H_2O located at $\nu = 5190$ cm^{-1} and $\nu = 3617$ cm^{-1}, respectively.

1. Introduction

Among a wide variety of the chalcogenides, arsenic selenides and arsenic sulfides are amorphous semiconductors particularly exploited and studied because of their interesting properties, which open prospective opportunities of various applications in optics, electronics and optoelectronics (optical elements and memories, optical sensors, non-linear optical devices, holographic elements, IR telecommunications, biosensing, signal processing, and photonic applications [1-3].

Even more interesting to study the chalcogenides doped with metal impurities, which alter the physico-chemical, electrical and optical properties [4-6]. It was shown that the Sn impurity introduced in the As_2Se_3, AsSe, and Sb_2S_3 glass network reduces the photodarkening effect [4, 5, 7]. Tin containing chalcogenides showed the some deviation in behavior due to modification in the local ordering of the host chalcogenide matrix after the tin incorporation, which was observed in the bulk glasses as well as in the corresponding thin films [7, 8]. For numerous of applications, the mechanical behavior is a one of important characteristic of the material [9-11].

In the present paper we have combined the experimental results of several studies of the bulk glasses samples $(As_4S_3Se_3)_{1-x}:Sn_x$ containing Sn ($x = 1 \div 10$ at.%), where the aims are: 1 – to determinate the microhardness and Young's module of different content x of Sn of the studying samples; 2 – to analyze the changes in medium range order (MRO) structure by X-ray diffraction method; 3 – to study of the optical transmission spectra.

2. Devices and materials

The bulk chalcogenide glasses $(As_4S_3Se_3)_{1-x}:Sn_x$ ($0 \le x \le 0.1$) were prepared from the elements of 6N (As, S, Se, Sn) purity by a conventional melt quenching method. The starting components elements $As_4S_3Se_3$ and Sn were mixed in quartz ampoules and then evacuated to pressure of $P \sim 10^{-5}$ torr, sealed and heated to temperature T=900 °C at the rate of 1 °C/min. The quartz tubes were held at this temperature for 48 hours for the homogenization and then slowly quenched in the furnace.

For the all measurements of the bulk samples were prepared the plan parallel plates of thickness about d =2÷3.5mm, and polished. Experiments were carried out to room temperature. Indentation were made with CSM Indentation Testers (Ultra Nano, Nano and Micro; with max load P=100 mN; loads resolution 0.001 μN) with software. With it automatically were computed hardness (Hv) and Young's modulus (E). The X-ray diffraction (XRD) measurements were performed on DRON-UM1 diffractometer with *Fe-Kα* radiation (λ=1.93604 Å), with Mn filter by $\theta/2\theta$ scanning method. For optical transmission spectra measurements, a UV/VIS (λ = 300÷800 nm), the 61 NIR (λ = 800÷3500 nm) Specord's CARLZEISS Jena production and Spectrum 100 FTIR Spectrometer (PerkinElmer) (λ = 1280÷25000 nm) were used.

3. Experimental and results.

Microhardness measurements

The operating principle of the tester is as follows: an indenter diamond tip, normal to the sample surface, is driven into the sample by applying an increasing load (P=100mN) up to some preset value. The load is then gradually decreased until partial or complete relaxation of the material occurs. After removal of the load is measured diagonal length, imprint *d1* and *d2*. The offset of diagonal tip was < 0.25 μm and the load resolution was 0.001N. To avoid overlapping of surface stresses developed around neighboring indentations the separation between indentation diagonals was kept more than ten times the diagonal length of indentation impressions. The dimensions of both diagonals d made at a particular load P were measured, and the average diagonal d was calculated [9]. The value of microhardness HV was computed from the $P(d)$ data using the standard well-known relation:

$$HV = kP/d2, \quad (1)$$

where k is a geometrical conversion factor for the indenter used (k = 0.1891):

$$k = 1/g(2\sin 136°/2), \quad (2)$$

where g is a acceleration of gravity, 136° is an angle between its opposite faces of piramidas tip. The average

values of indentation diagonal d and microhardness HV for at least 10 indentations were used in the analysis of indentation size effect and hardness measurements. In the case of the Vickers indenter when P is taken in N and d in μm.

Fig. 1 shows the microhardness dependence of the tin content in bulk samples of As_4S_3, As_4Se_3, $As_4S_3Se_3$, and $(As_4S_3Se_3)_{1-x}$:Sn_x (x = 1 ÷ 10 at.%). It is seen, that addition of tin in host material has little effect on the character of the curve, which is on microhardness. Although there is observed some decline and then increasing of microhardness. Bat in general, the hardness varies around one value H_{middle} = 1282 MPa.

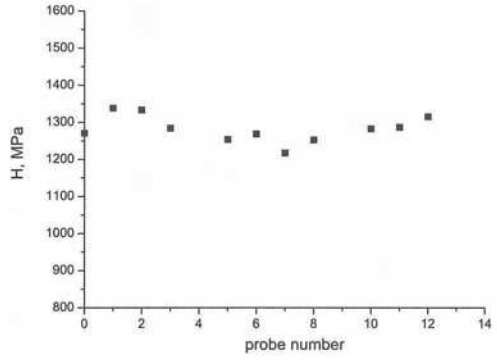

Fig. 1. Compositions dependence of microhardness of the samples: 0 - As_4S_3; 1 - As_4Se_3; 2 - $As_4S_3Se_3$; 3 ÷ 13 - $(As_4S_3Se_3)_{1-x}$:Sn_x (x= 1 ÷ 10 at.%) .

Fig. 2 shows the Young's module dependence of different content x of Sn. In this case the some slight decline in elasticity is observed. That is, the material becomes brittle.

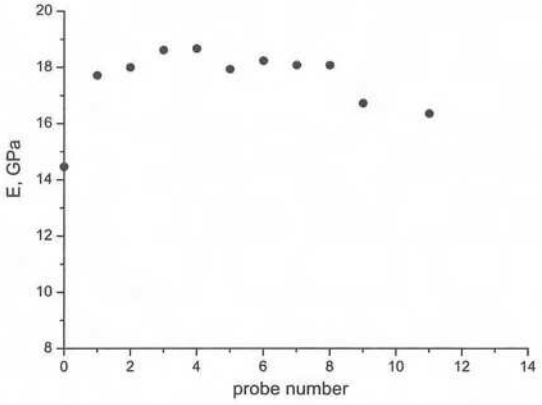

Fig. 2. Compositions dependence of Young's modulus of the samples: 0 - As_4S_3; 1 - As_4Se_3; 2 - $As_4S_3Se_3$; 3 ÷ 13 - $(As_4S_3Se_3)_{1-x}$:Sn_x (x = 1 ÷ 10 at.%).

Figure 3 represent the imprint on the surface of the diamond tip on some $(As_4S_3Se_3)_{1-x}$:Sn_x sample at load P=100 mN. Figure 4 represent the depth dependence of the load and unload values on chalcogenide samples of As_4S_3, As_4Se_3, $As_4S_3Se_3$, and $(As_4S_3Se_3)_{1-x}$:Sn_x (x = 0 ÷ 10 at.%).

X-Ray diffraction .

Using the X-Ray Diffraction method were obtained the diffraction patterns in the range of diffraction angles 2θ from 10° to 80° (θ is the Bragg angle) for the chalcogenide glasses As_2S_3, As_2Se_3, $As_4S_3Se_3$, and $As_4S_3Se_3$:Sn_x (x = 0.01, 0.02, 0.04, 0.06, 0.07 и 0.10).

Fig. 3. Example of imprint on the surface of the diamond tip on $(As_4S_3Se_3)_{1-x}$:Sn_x samples at load P=100 mN.

Fig. 5 indicates the angular distribution of X-Ray diffraction intensity for As_2S_3, As_2Se_3, and $As_4S_3Se_3$ prepared glasses. The position of the First Sharp Diffraction Peak (FSDP) for As_2S_3 is 2θ=22.47° and increase up to 2θ=24.60° for As_2Se_3. For the intermediate composition $As_4S_3Se_3$ the maximum of the FSDP is situated at 2θ=23.00° (Fig.5). These spectra represent a sum of diffraction patterns of izostructural vitreous As_2S_3 and As_2Se_3 with three broad lines of diffractograms and which are similar to the unvelope of the rounded lines of the spectra of crystalline As_2S_3 and As_2Se_3.

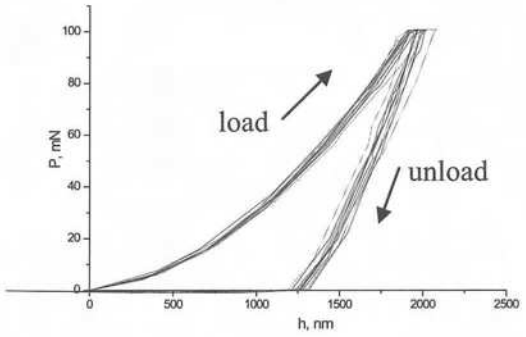

Fig. 4. Plots of depth dependence of the load and unload values on chalcogenide samples of $(As_4S_3Se_3)_{1-x}$:Sn_x

It can be assume about the microcrystalline state of the investigated glasses – existense of domains with ordered structure with dimensions about 15 – 20 Å. Previously a analogy between the structure of vitreous and crystalline states of As_2S_3 was vindicated by short-range order investigations – interatomic distances and coordination numbers – with the add of the radial distribution function [12].

The carefull investigations of the FSDP of viteous As_2S_3 and As_2Se_3 show that they have a similar structure [13]. According to [13], the first coordination spheres

(first order neighbour position) of a central atom in the structure is r_1=2.414 Å for As_2Se_3, and r_1=2.306 Å for As_2S_3, respectively. The second coordination spheres (second order neighbour position) of a central atom in the structure is r_1=3.625 Å for As_2Se_3, and r_1=3.475 Å for As_2S_3, respectively.

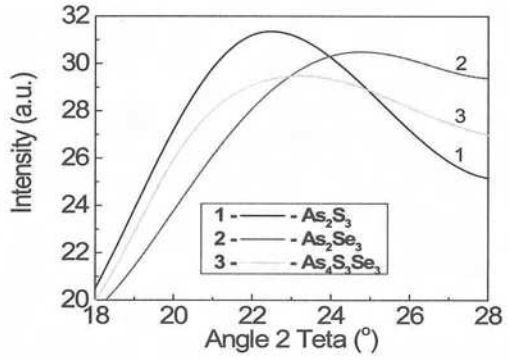

Fig.5. First sharp diffraction peak (FSDP) in the X-ray diffraction patterns of As_2S_3 (1), As_2Se_3 (2), and $As_4S_3Se_3$ (3).

It was established that between As_2S_3 and As_2Se_3 layers act Van der Waals forces with a reduced covalent component. The interaction forces between layers are hundred times weaker than the binding forces between the layers.

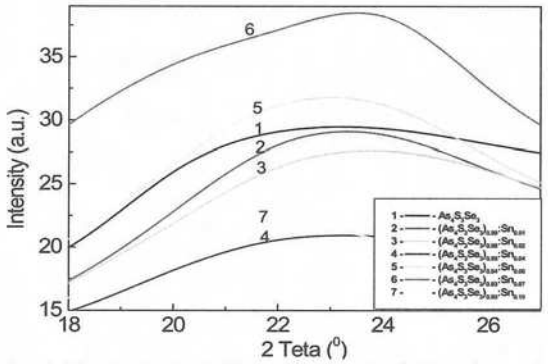

Fig.6. First sharp diffraction peak (FSDP) in the X-ray diffraction patterns of $As_4S_3Se_3$ (1), $(As_4S_3Se_3)_{0.99}$:$Sn_{0.01}$ (2), $(As_4S_3Se_3)_{0.98}$:$Sn_{0.02}$ (3),$(As_4S_3Se_3)_{0.96}$:$Sn_{0.04}$ (4), $(As_4S_3Se_3)_{0.94}$:$Sn_{0.06}$ (5), $(As_4S_3Se_3)_{0.93}$:$Sn_{0.07}$ (6), $(As_4S_3Se_3)_{0.90}$:$Sn_{0.1}$ (7).

According the [13], the structure of the glasses represent as an interliking of As-S_3 and As-Se_3 pyramids that forms rings with 6 units. The arsenic atoms are situated at the top of the pyramid, while the chalcogen atoms form the basis.As was shown, the crystalline semiconductors are characterized by long-range order (LRO), i.e. there is a good correlation between the position in the network, of the each two atoms, that can't be said about the non-crystalline semiconductors [14, 15]. For non-crystalline semiconductors, there is only short-range order (SRO), which belongs to the individual atoms in the first coordination sphere. As in chalcogenide glasses range order can be extended to several interatomic distances, the new concept of the average order was introduced (MRO).

The Sn concentration in the mixted glasses $As_4S_3Se_3$:Sn_x essentially don't change the shape of the FSDP of the X-ray diffraction patterns (Fig. 6).

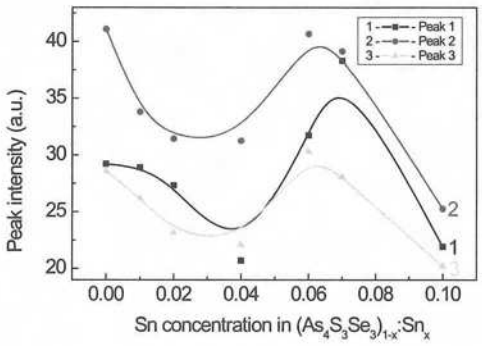

Fig.7. Dependence of the angular position of the diffraction peaks vs. concentration of tin in the some chalcogenide glass $As_4S_3Se_3$:Sn_x.

In general, the diffraction patterns of the $As_4S_3Se_3$:Sn_x glasses are similar and form three wide lines, the maxima of which correspond to the interlayer distances d~4.8 – 2.8 – 1.7 Å. As in the case of As_2Se_3:Sn_x [16], the angular position of the FSDP in the $As_4S_3Se_3$:Sn_x slightly depend on the Sn concentration. Fig.7 shows the dependences of the peaks intensities vs. concentrations of tin of the three diffraction peaks of chalcogenide glass $As_4S_3Se_3$:Sn_x situated at 2θ~22÷24°, 2θ~40÷42°, and 2θ~62÷70°, respectively.

The intensity of the FDSP shows a non-linear behavior with the different amount of doping of Sn. The maximum intensity is reached around 6 at.% Sn in $As_4S_3Se_3$:Sn_x, while in the case of As_2Se_3:Sn_x the maximum intensity is situated at the tin concentration at ~ 2 at.% Sn. The similar behavior was found for the 2-nd and the 3-rd difraction peaks.

According to [12], when Sn is added in ChGS like As2Se3 or As2S3, due to the tetrahedral disposal of the sp3 bonds in the chalcogen the dopant atom inserted in the network increases the thickness of the layered configuration as revealed by the significant shift of the FSDP towards lower angles. This insertion corresponds to the introduction in the glass network of the structural units of the type $SnSe_2$ or SnS_2, and the same fact was confirmed by the Mössbauer spectroscopy experiments [3].

The transmission spectra.

The mid-IR transmission spectra of As_2S_3 and some $As_4S_3Se_3$:Sn_x bulk glasses are shown in Fig. 8 and, as in the case of vitreous As_3S_3 doped with metals [16], are characterized by several well-resolved absorption bands. For vitreous As_2S_3, these bands are located at frequencies of ν = 5190 cm^{-1} (S-H), ν = 3617-3522 cm^{-1} (H_2O), ν = 2482 cm^{-1} (S-H), ν = 1857 cm^{-1} (As-H), ν = 1597 cm^{-1} (H_2O), and ν = 1003 cm^{-1} (As_2O_3. The characteristic absorption bands for pure As_2S_3 at ν = 5190, 3617, 3522, 1857, and 1597 cm^{-1} are significantly reduced upon doping with Sn. At the same time, for the $[(As_2S_3)_{0.5}$:$(As_2Se_3)_{0.5}]_{0.98}$:$Sn_{0.02}$ glass, additional absorption bands appear at ν = 5190 cm^{-1} 3194, 2026, and 1493 1500 cm^{-1}.

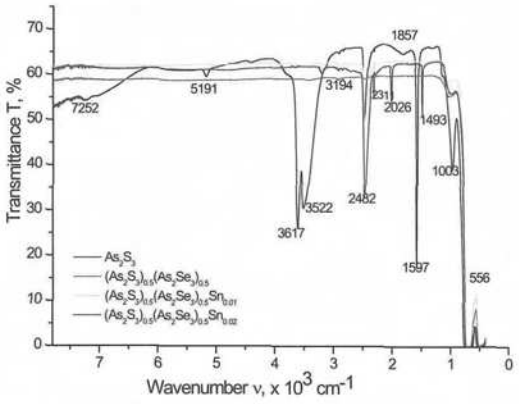

Fig. 8. Transmission spectra of some bulk samples of $As_4S_3Se_3$:Sn_x glasses.

The observed changes upon doping in the mid infrared region are most likely related to interactions of a portion of the introduced metal ion impurities with the inherent impurities of the host glass, such as hydrogen and oxygen atoms. These interactions result in the reduction of the relative intensity of bands associated with O-H, S-H, As-O, and As-H bonds in the parent glass.

4. Conclusion

Was establish that addition of Sn atoms in chalcogenide glass matrix essentially decrease the elasticity of this material or increase the hardness at some tin concentrations. This presumably due to their incorporation in the existing microvoids, restructuring of the polymer network and increasing cross-linking of the polymer chains, that leading to the formation of more compact structure

The doping of $As_2(S, Se)_3$ chalcogenide glass with tin impurities essentially reduces the absorption bands of S-H (Se-H) and H_2O located at ν = 5190 cm^{-1} and ν = 3617 cm^{-1}, respectively.

5. Acknowledgments

The author is kindly grateful to to Drs. D.F. Felix, and A.Yu. Meshalkin for some optical measurements; Dr. G.F.Volodina for X–ray diffractions measurements. The work was supported by the national project no. 11.817.05.03A and WFS Grant.

6. References

[1] Zakery A., Elliot, S.R., *Optical Nonlinearities in Chalcogenide Glasses and Their Applications*, Springer, Berlin-Heidelberg-New York, 2007.

[2] Andriesh, A.M., Iovu, M.S., Shutov, S.D., Chalcogenide Non-Crystalline Semiconductors in Optoelectronics, J. Opt. Adv. Mater., 4, 631, 2002.

[3] Nemec, P., Jedelsky, J., Frumar M. Štábl, Vlček M., *Structure, thermally and optically induced effects in amorphous As_2Se_3 films prepared by pulsed laser deposition*, J. Phys. Chem. Solids, 65(7), 1253, 2004.

[4] Iovu, M., Shutov, S., and Popescu, M., *Relaxation of photodarkening in amorphous AsSe films doped with metals*, J. Non-Cryst. Solids, 924, 2002.

[5] Boolchand, P., Georgiev, D., and Iovu, M., *Molecular structure and quenching of photodarkening in As2Se3:Snx amorphous filmschalcogenide,* Lett., 2(4), 27, 2005.

[6] Iovu, M., Boolchand, P., and Georgiev, D., J. Optoelectron. Adv. Mater., 7(2), 763, 2005.

[7] Iovu, M., Harea, D., and Colomeico E., J. Optoelectron. Adv. Mater., 10(4), 862, 2008.

[8] Iaseniuc, O. V., *Optical properties of some [(As2S3)0.5:(As2Se3)0.5]1-x:Snx chalcogenide glasses*, Moldavian Journal of the Physical Sciences, 11(1-2), 60, 2012.

[9] Yong Yee Lim, Munawar Chaudhri, M., *Indentation of elastic solids with a rigid Vickers pyramidal indenter*, Mechanics of Materials, 38, 1213, 2006.

[10] Trunov, M.L., Bilanich, V.S., *Photoplastic phenomena in chalcogenide glasses*, J. Optoelectron. Adv. Mater., 5(5), 1085, 2003.

[11] Yannopoulos, S.N., Trunov, M.L., *Photoplastic effects in chalcogenide glasses*: A review, Phys. Status Solidi B 246(8), 1773, 2009.

[12] Tatariniva, L., *The structure of amorphous solids and liquids*. M., «SCIENCE», 151, 1983.

[13] Popescu, M., Andries, A., Ciumas, V., Iovu, M., Şutov, S., Ţiuleanu, D., *Physics of chalcogenide glasses,* Science Bucuresti, Science Chisinau, 1996.

[14] Popescu, M., *Medium range orders in chalcogenide glasses*, In: Physics and Applications of Non-Crystalline Semiconductors in Optoelectronics, Eds. A. Andriesh & M. Bertolotti, 36, 215, 1996.

[15] Popescu, M., Tudorica, F., Andriesh, A., Iovu, M., Shutov, S., Bulgaru, M., Colomeyco, E., et.al., *Structure and electrophysical properties of tin doped arsenic selenide glasses*, Physics and Engin, 3, 3, 1995.

[16] Iovu, M., Shutov, S., Andriesh, A., Kamitsos, E., Varsamis, C., Furniss, D., Seddon, A., Popescu, M., *Spectroscopic studies of bulk As_2S_3 glasses and amorphous films doped with Dy, Sm and Mn*, J. of Optoelectronics and Advanced Materials, 3(2), 443, 2001.